Astron. Astrophys. 344, 511–520 (1999)

ASTRONOMY AND ASTROPHYSICS

A homogeneous temperature calibration for K and M giants with an extension to the coolest stars⋆

A. Richichi[1], **L. Fabbroni**[2], **S. Ragland**[1], **and M. Scholz**[3]

[1] Osservatorio Astrofisico di Arcetri, L.go Enrico Fermi 5, I-50125 Firenze, Italy
[2] Dipartimento di Statistica, Viale Morgagni 59, I-50134 Firenze, Italy
[3] Institut für Theoretische Astrophysik der Universität Heidelberg, Tiergartenstrasse 15, D-69121 Heidelberg, Germany

Received 6 October 1998 / Accepted 16 December 1998

Abstract. In this paper we present a new estimate of the effective temperatures of 32 giant stars in the spectral range K0 to M10. The sample includes also 4 Mira stars. The temperatures are based on a homogeneous set of angular diameters obtained by our group by the technique of lunar occultations, and using a photometric and spectroscopic coverage with a combination of original measurements and literature data. Most of this basic material had been presented in previous papers, but in the present work we derive improved effective temperatures by using for the first time a grid of numerical center-to-limb darkening models. We use this revision to derive a new calibration of the effective temperature of K and M giant stars, which has the advantage of being based on only one, highly homogeneous set of data (while previous calibrations often used mixed data sets). The resulting calibration is extended to the coolest stars, reaching for the first time M9 for the non-Mira stars, and M10 for the Mira stars. In this latter case the calibration does not account for pulsation phase variations and is only tentative. In the region of overlap with previously existing calibrations, we find a largely satisfactory agreement, although some differences exist and are discussed. In particular, it appears that the calibration of the effective temperature of cool Mira stars requires additional observational as well as theoretical effort. Seven of the stars in our sample appear to exhibit an effective temperature that departs significantly from the mean relation (≈ 900 K cooler between K1 and M8), and no simple explanation in terms of possible bias or experimental error could be found.

Key words: infrared: stars – stars: circumstellar matter – stars: fundamental parameters – stars: late-type – occultations

1. Introduction

The knowledge of the effective temperature of stars is of fundamental importance in astronomy for various reasons. Firstly, it provides a fundamental test for stellar models, involving aspects of stellar structure, composition and evolution. The effective temperature of a star, deduced from its measured angular diameter and bolometric flux, is completely independent from the distance to the star, and therefore it represents a powerful method to test theoretical models on a very large and varied number of stars. Secondly, the calibration of effective temperatures with spectral type (possibly complemented by luminosity class and chemical composition) is of fundamental importance for investigations involving stellar populations, and as such it finds extensive use in galactic and extragalactic studies. Finally, recent accurate parallax measurements, such as those obtained by the Hipparcos satellite, are beginning to permit a direct conversion of many angular diameters into linear sizes, opening a new point of view on stellar studies.

Empirically, it has long been established that the effective temperatures of spectral types similar to or hotter than solar can be well described by a simple temperature–color relation (Barnes & Evans 1976): although based on relatively few measurements, this calibration seems very reliable and leads to accurate predictions. For spectral types K and cooler ($T_{\rm eff} \lesssim 4500$ K), however, the situation is more complex. Initial attempts to define a relationship between temperature and visual color indices were less successful for cooler stars, mainly because of the presence of broad molecular bands in the V, R and I filters. Instead, it was necessary to push studies of the diameters and photometric coverage for these stars into the near–infrared (NIR). Ridgway and collaborators (Ridgway et al. 1980, R80 hereafter) were the first to present a calibration for stars in the spectral range K0 to M6, based on lunar occultation (LO) results. Their results showed a rather large scatter, but it is remarkable that the average temperature derived for each spectral type has remained essentially valid until now. About a decade later, calibrations based on long–baseline interferometry (LBI) results began to appear (Di Benedetto & Rabbia 1987), showing a substantial agreement with the R80 relationship. Later on, additional results by LBI extended it to M7 (Dyck et al. 1996, D96 hereafter) and M8 (Perrin et al. 1998, P98 hereafter). We note that all recent calibrations have relied at least partially on previous LO results.

Send offprint requests to: A. Richichi (richichi@arcetri.astro.it)

⋆ Based on observations collected at TIRGO (Gornergrat, Switzerland), at Calar Alto (Spain) and at the European Southern Observatory in La Silla (Chile). TIRGO is operated by CNR – CAISMI Arcetri, Italy. Calar Alto is operated by the German-Spanish Astronomical Center.

With this paper, we try to improve the existing situation in the field of effective temperature calibrations in three respects:

a) We present a calibration that extends to reach the coolest non–Mira giant stars, including the subtype M9, which had never been sampled before. Additionally we present data for Miras in the range M8–M10: this also represents a new extension to the present calibrations, although in this case our conclusions are necessarily of a tentative nature, as explained in Sect. 4.

b) Our results are based entirely on our own data for angular diameters. This ensures that all the details of data acquisition and analysis are homogeneous throughout our data set. Previous work has shown that our angular diameter determinations, thanks also to the developments introduced in the LO data analysis techniques, are in general significantly more accurate than those used in the R80 calibration. Also, for the collection of photometric and spectroscopic data, we have tried as much as possible to obtain original measurements and to include the effects of variability, which are quite significant, especially for the coolest spectral types.

c) For the first time we present a consistent use of numerical center-to-limb variation (CLV) models in the LO data analysis. We express our angular diameters in terms of a physically meaningful quantity (namely, the Rosseland radius, defined by the distance from the star's center to the layer of unit Rosseland optical depth) and consequently derive effective temperatures that can be directly compared to model predictions.

2. Observational database

The foundation of this paper is a database of angular diameter results that we have obtained by means of the LO technique over more than a decade at the TIRGO, La Silla and Calar Alto observatories. These results have been published mostly as uniform disk (UD) values by our group in Arcetri and by several collaborators at other institutes. A total of about 80 stars have been resolved, of which 32 have characteristics which are useful for the purpose of this paper, in which we concentrate exclusively on giant stars of normal composition (thus excluding supergiants and carbon stars). The remaining stars in our database do not have enough information on their spectral types and bolometric fluxes, or belong to other classes and will be discussed in separate papers. The angular diameters are listed in Table 1, and they differ slightly from the previously published values because we have recomputed them including limb darkening based on CLV numerical models as explained in Sect. 3.1. The sample consists actually of 34 measurements, since in two cases (RX Cnc and DW Gem) repeated LO events were observed. Note that RX Cnc is reported with a mean spectral type of M6, although in the original paper by Richichi et al. 1988 it was suggested that a spectral type variation might have occurred between the two LO measurements. The choice of reporting a common mean spectral type is consistent with the associated uncertainties and does not affect significantly the calibration discussed in Sect. 4. In Table 1, the first two columns report the source identification and the spectral type (see also Sect. 3.3). Column (3) reports the variability class, whose symbols are defined in the General Catalogue of Variable Stars (GCVS, Samus 1990) and in particular, L denotes the slow irregular variables, SR the semi–regular variables, and M the Mira stars. The symbol NSV is used for sources listed in the catalogue of new suspected variables (see GCVS above). Column (4) lists the uniform–disk diameters, and Column (5) lists the references to the papers where the occultation data were originally published. All the LO observations on which this paper is based were recorded in the NIR using broad band K and L filters. Note that in the case of IRC+20097, the LO data were recorded while this paper was being written and the resulting K–band angular diameter is published here for the first time. Columns (6) and (7) list the adopted values of interstellar extinction to the stars and the the spectral bands covered by our spectroscopic observations (see Sect. 3.2 and 3.3). Column (8) lists the bolometric fluxes and their errors, to be discussed in Sect. 3.2. Column (9) lists the new estimates of the limb–darkened diameters in the $\tau_{\rm Ross}$=1 assumption (see Sect. 3.1), and Column (10) lists the corresponding effective temperatures which are the basis of our calibration as discussed in Sect. 4.

In parallel to the LO program, we have undertaken an effort over about a decade to collect photometry of a significant fraction of this sample, mostly in near-IR bands, but partly also in the visual range. This was made necessary for a correct evaluation of the bolometric fluxes, as explained in Sect. 3.2. Finally, a similar effort was undertaken also to obtain near–IR spectra for a number of stars for which this information was not entirely satisfactory (see Sect. 3.3). A large part of the photometry has already been published (see Richichi et al. 1998b and references therein), while most of the spectroscopy has been collected and evaluated explicitly for this paper. We do not show in printed form the full database of the photometric and spectroscopic measurements, but they are available upon request in electronic format.

Since most of the sources in our sample were dealt with in previous papers, we do not present here any detailed individual discussion. Information on cross–identifications, magnitudes, distances, and in some cases binarity, can be extracted from our previous work as noted above, as can details of the telescopes and instruments used for the observations. Details about the sensitivity of the LO techniques, including a statistical discussion of the magnitudes, angular resolution, scattered light background can be found in previous works and in particular they were discussed for the specific case of the TIRGO telescope by Richichi et al. 1996b.

3. Definitions and bias in deriving effective temperatures

Before turning to the effective temperatures derived on the basis of our observational database and the corresponding $T_{\rm eff}$–spectrum calibration, it is necessary to examine some possible sources of error and bias. The calibration involves the measurement of three quantities: an angular diameter, a bolometric flux (both needed for the effective temperature determination), and the spectrum to which the temperature should be associated. Although these quantities are simple to identify and their

Table 1. Summary of data and results (see text).

(1) Source	(2) Sp.	(3) Var. type	(4) ϕ_{UD} (mas)	(5) Ref.	(6) A_v (mag)	(7) Spectral band	(8) Bolom. flux (10^{-10} Wm^{-2})	(9) ϕ_{LD} (mas)	(10) T_{eff} (K)
IRC−20550	K0		1.43 ± 0.15	5,7	0.0		3.88 ± 0.19	1.44 ± 0.15	4869 ± 262
IRC+20074	K0	NSV	2.69 ± 0.18	8	0.0		12.83 ± 0.84	2.72 ± 0.18	4778 ± 177
IRC+20097[b]	K1		3.76 ± 0.21		0.7		4.10 ± 0.22	3.80 ± 0.21	3038 ± 94
IRC+20141[b]	K2		2.11 ± 0.09	6,7	1.2	H	2.78 ± 0.14	2.13 ± 0.09	3683 ± 90
IRC+10007	K4		3.91 ± 0.17	4	0.4		14.33 ± 0.28	3.95 ± 0.17	4075 ± 90
IRC+20133[b]	K4		2.81 ± 0.09	7	0.8	H	4.76 ± 0.20	2.84 ± 0.09	3649 ± 69
IRC+20071[b]	K5		2.71 ± 0.15	6,7	0.0	H,K	3.03 ± 0.10	2.74 ± 0.15	3319 ± 95
IRC+10024[a]	M2		3.20 ± 0.17	4	0.0		6.59 ± 0.14	3.26 ± 0.17	3695 ± 98
IRC−30253[a]	M2		3.75 ± 0.35	4	0.4		9.22 ± 0.18	3.82 ± 0.36	3712 ± 177
IRC+20067[a,b]	M2		3.68 ± 0.24	8	0.6	H	1.46 ± 0.08	3.75 ± 0.24	2363 ± 83
IRC+20155[a,b]	M2	NSV	3.89 ± 0.12	8	0.3	H,K	2.25 ± 0.11	3.96 ± 0.12	2562 ± 49
IRC+10034[a]	M4		3.64 ± 0.07	7	0.2	K	6.67 ± 0.40	3.72 ± 0.07	3469 ± 61
IRC−20356[b]	M4		3.02 ± 0.24	8	0.7		1.44 ± 0.16	3.09 ± 0.25	2593 ± 129
IRC−20510[a]	M4	SRb	8.09 ± 0.27	8	0.0		34.07 ± 3.06	8.27 ± 0.28	3497 ± 98
AX Sco	M5	SRb	4.49 ± 0.50	3	0.5		9.64 ± 0.74	4.61 ± 0.51	3416 ± 201
SW Gem	M5	SRa	2.80 ± 0.09	7	0.0		3.12 ± 0.19	2.87 ± 0.09	3267 ± 72
AX Gem[a]	M5	Lb	3.02 ± 0.07	7	0.0	K	3.86 ± 0.29	3.09 ± 0.07	3320 ± 73
RX Cnc	M6	SRb	4.23 ± 0.09	1	0.0	H,K	6.83 ± 0.49	4.31 ± 0.10	3242 ± 70
			3.18 ± 0.12					3.28 ± 0.10	3716 ± 88
AFGL 5196S	M6		2.61 ± 0.30	3	0.3		4.14 ± 0.38	2.67 ± 0.31	3634 ± 228
T Ari[a]	M6	SRa	7.08 ± 0.13	7	0.0	H,K	15.79 ± 0.73	7.26 ± 0.13	3080 ± 45
IRC−20307[a]	M6		2.05 ± 0.16	7	1.3		2.22 ± 0.34	2.10 ± 0.16	3507 ± 190
Z Cnc	M6	SRb	4.26 ± 0.31	8	0.0	H,K	6.99 ± 0.40	4.37 ± 0.32	3238 ± 128
DV Tau	M6	Lb	3.79 ± 0.13	8	0.2	K	4.97 ± 0.32	3.89 ± 0.13	3152 ± 73
RS Cap	M6	SRb	7.75 ± 0.67	4	0.0		30.89 ± 3.25	7.95 ± 0.69	3481 ± 177
DW Gem[a]	M7	Lb	5.92 ± 0.11	4	0.0		13.28 ± 0.76	6.09 ± 0.11	3220 ± 56
			6.24 ± 0.30					6.41 ± 0.31	3139 ± 88
IRC−20578[a]	M7		3.21 ± 0.11	8	0.5		2.86 ± 0.27	3.30 ± 0.11	2980 ± 88
R Leo	M8	M	33.0 ± 1.3	2	0.0		146.9 ± 12.7	33.99 ± 1.34	2486 ± 73
AFGL 5151S[b]	M8	NSV/M?	3.38 ± 0.30	3	1.2		0.77 ± 0.05	3.50 ± 0.31	2084 ± 97
AW Tau	M9	M	3.13 ± 0.79	4	0.7	H,K	0.88 ± 0.05	3.23 ± 0.82	2244 ± 293
AFGL 2061[a]	M9	M:	5.93 ± 0.30	3	0.4		3.91 ± 0.25	6.19 ± 0.31	2354 ± 71
IRC−20444[a]	M9		4.54 ± 0.06	8	0.7		3.55 ± 0.65	4.69 ± 0.06	2638 ± 130
RU Ari[a]	M10	M	4.10 ± 0.38	8	0.6		1.09 ± 0.08	4.24 ± 0.39	2066 ± 102

[a] Stars used to derive the limb darkening factor (see Sect. 3.1)
[b] Stars not used in the T_{eff} calibration (see Sect. 4).
References: (1) Richichi et al. 1988. (2) Di Giacomo et al. 1991; (3) Richichi et al. 1992a; (4) Richichi et al. 1992b; (5) Richichi et al. 1996a; (6) Richichi et al. 1997; (7) Richichi et al. 1998a; (8) Richichi et al. 1998b.

measurement may seem intuitive, there are in fact some complications related to their definition and to the intrinsic nature of the target stars.

3.1. Angular diameters and limb darkening

The effect of limb darkening on an occultation light curve is small, and the amount of limb darkening can be inferred directly from the data only in the case of light curves obtained with very good signal–to–noise ratio (e.g., Richichi & Lisi 1990). More typically, one assumes either a uniform or a fully darkened disk in the data reduction, and applies appropriate scaling factors later in converting the resulting non-physical angular diameter to a model-related physical quantity such as a limb–darkened diameter. Such factors are usually adopted from standard theoretical models, which however do not always cover adequately the full range of temperatures and luminosities.

It is important to stress that in the case of noticeably extended atmospheres like those of the late M giants which are discussed here, the CLV curve has no real edge corresponding to a physical limit in the photospheric extension (e.g., Baschek et al. 1991, Scholz 1997). A meaningful diameter definition, as far as effective temperatures are concerned, must be derived with respect to the model-predicted position of a specific optical depth layer. Throughout this paper we shall refer implicitly to diameters and effective temperatures derived with respect

to $\tau_{\rm Ross}$=1. Limb darkening affects the measurement of stellar diameters of cool stars mostly at visual wavelengths, which are severely affected by molecular band absorption. In the NIR continuum, the effect is typically around or below the 5% level (Schmidtke et al. 1986), and publications often report the uniform disk diameter or a limb–darkened diameter with nominal corrections.

While this can be justified in the case of individual results where other sources of errors can be dominant, for a temperature calibration it is necessary to understand and account for limb darkening effects in the best possible way. We note that R80, which still represents the only work entirely based on LO, combined results from several authors: although an effort was made to convert these results into limb–darkened diameters, inevitably it was impossible to do this in a homogeneous way, if only because of the different wavelengths of observation. P98 fitted their interferometric data with models published in the literature for late-type giants in the K band and suggested a scaling factor of 1.035 to obtain limb–darkened disk diameter from uniform disk diameter. Earlier, D96 had suggested a scaling factor of 1.025 from their visibility data combined with the model atmospheric calculations.

We are in a position to exploit a database of homogeneous results and we have made an effort to include limb darkening in our analysis by means of a novel approach. We used a grid of numerical CLV models for our specific bandpasses computed from the non-Mira M giant models of Bessell et al. (1989a, 1991). This grid covers a range of masses and luminosities for $T_{\rm eff}$ between 2500 K and 3800 K. Computational procedures and general CLV properties are described in a recent work by Hofmann & Scholz 1998. For each point in the grid, we generated a numerical strip–integrated brightness profile. This was normalized in units of the Rosseland radius, whose position on the CLV curve was taken from the model. A given occultation light curve was then analyzed using the whole grid of numerical models (a total of 22). For each star, the model yielding the best result was selected, using also the constraint of expected luminosity based on the estimated distance. The resulting angular diameter was used to derive a preliminary effective temperature and if this differed significantly from that of the model, the procedure was iterated. One or two iterations were always sufficient.

This was repeated for a sample of 14 light curves (see Table 1) of good quality spanning the range of available model temperatures. Two Miras are included in this sample, but this is justified at the end of this subsection. The result is shown in Fig. 1, where it can be seen that the limb–darkened to uniform–disk factor can be estimated with good accuracy. A dependence on the spectral class is also evident, ranging from $\lesssim$2% for early M to 3–4% at the end of the M class. For our purposes, it is not necessary to estimate the correction factor with more than 0.5% accuracy (equivalent to about 15 K) and we used a simple linear fit to the data of Fig. 1. We have chosen to represent the spectral classes at equal intervals. This is arbitrary, but on the other hand the correlation and the adopted fit are sufficiently convincing that we felt no need to seek representations based on more complicated physical justifications. This subject will be discussed further in Sect. 4.

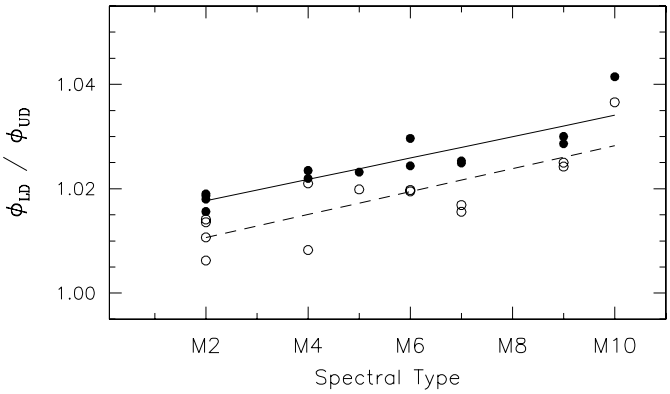

Fig. 1. The conversion factor between limb–darkened and uniform disk diameter derived, for a sample of light curves (dots) according to the methods described in the text. The solid points are for the case $\tau_{\rm Ross}$=1, while the open points are for the case $\tau_{\rm cont}$=1. The solid and dashed lines respectively are the adopted mean relations in the two cases.

We applied the scaling factor discussed above to all the uniform–disk diameters, and the corresponding limb–darkened diameters are also listed in Table 1. Note that a constant factor of 1.01 was applied to the K spectral types, which are not covered by the available numerical grid. These stars are less relevant for the extended calibration that we intend to derive.

While the effective temperature can be well defined using a Rosseland diameter, one must be aware that at very low temperatures the Rosseland radius relation may depend appreciably on modelling techniques and substantial deviations from monochromatic continuum diameters may occur (Hofmann & Scholz 1998, Hofmann et al. 1998). We therefore compared our Rosseland diameters with filter diameters referring to our continuum passbands. We carried out intensity-weighted filter integrations after Scholz & Takeda 1987, using the actual transmission curves of the K and L filters used in each LO observation. However, since opacities change little over the band width, these filter diameters are essentially monochromatic $\tau_{\rm cont}$=1 diameters. Fig. 1 shows that the difference in the resulting limb–darkened angular diameter is ≈ 0.7%, a very small value which implies almost negligible differences in the estimation of the effective temperature.

For the Miras, an extension of the CLV grid described above was in preparation at the time of writing (Hofmann et al. 1998). Although it was not possible to use such a grid in a systematic way, as we did for the non-Mira stars, we estimated that the differences to be expected in the Rosseland diameters between the two grids would be very small in our NIR filters. Since, furthermore, our Mira calibration is only tentative at the present stage (see Sect. 4), we systematically applied the limb darkening correction derived above to all stars in our sample including the four Mira variables. Note that two Miras are used in the fit shown in Fig. 1, which is then slightly biased but at a level not exceeding the stated accuracy of 15 K.

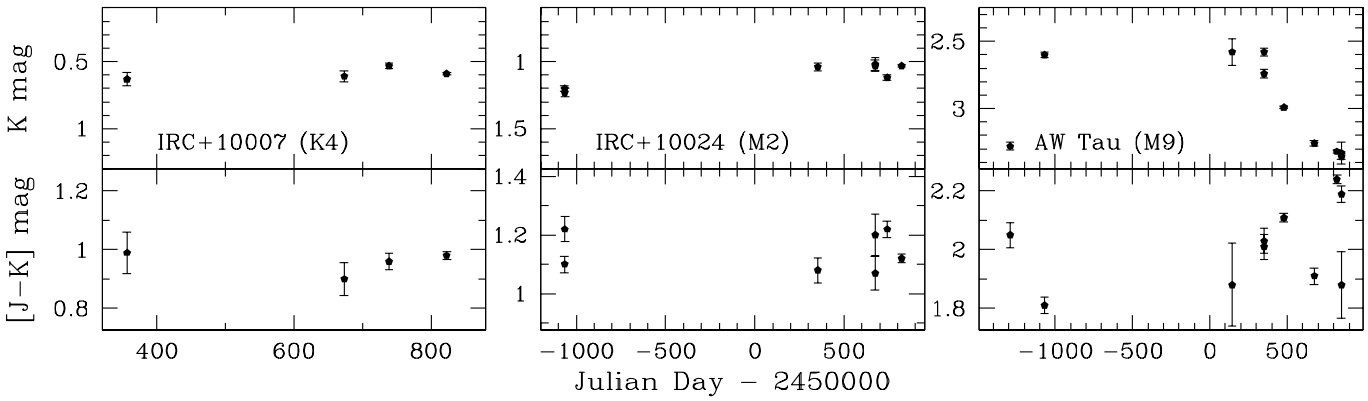

Fig. 2. Magnitude (*top panels*) and color (*lower panels*) light curves for three sources, representative of different class of variability. Note the different scales in the magnitude plots.

3.2. Bolometric fluxes in the presence of variability and extinction

The spectra of M giants, especially of the latest subclasses, depart significantly from a blackbody. In the absence of high resolution absolute spectra in the complete optical and NIR regions, we tried to overcome the problem by estimating the bolometric flux after rejection of those photometric bands which are severely affected by molecular absorption. Giants of type M5 and later show IR excess, and in this case an additional cooler blackbody component has been incorporated. In spite of the relatively weak dependence (1/4 power) of the effective temperature on the bolometric flux, the error associated with the latter is the limiting factor for a significant fraction of the stars in our sample, as found by Richichi et al. 1998b. The major sources of uncertainty in the bolometric flux are photometric variability and interstellar and/or circumstellar extinction, and we discuss them below.

Photometric variability in the visual and NIR is a rule rather than an exception in M giants. The amplitude of variability can be as large as a few magnitudes in the optical, but is considerably smaller in the NIR. The optical variability does not affect our bolometric flux estimation severely, since the optical flux contributes little to the total flux, and additionally those optical bands which are affected by molecular absorption bands are excluded from our fits. On the other hand, the small amplitude near–IR variability, if not properly taken into account, can bias the bolometric flux and hence the stellar effective temperature severely, since the Planck function peaks in the NIR for M giants.

In order to reduce the error involved in the bolometric flux due to NIR photometric variability, we have been carrying out a program of long term monitoring of our sample for several years. Three examples of photometric light curves are shown in Fig. 2, illustrating different situations of variability. The color variations are much smaller than the magnitude variations, at least for the K4 and M2 stars, indicating a relatively constant (color) temperature. The situation for the cool M9 star is more complex, indicating that more significant changes may occur in the photosphere of cooler stars during the variability cycle.

Our interest has been to establish the scatter in the photometric values and not the variability period or the phase, most of the stars being either semi-regular or irregular variables. Hence, we have not monitored these sources continuously but rather in an irregular way during available breaks in other programs. Nevertheless, our photometric data set is sufficient for some quantitative conclusions.

In particular, we note that when photometric measurements are available at several different epochs and are combined together incoherently, our fit yields a time–averaged bolometric flux which has a typical formal accuracy of ≈6%, which in turn implies a 1.5% error on the temperature. This result has been established using 12 representative cases of our sample, and this source of error is included in the values listed in Table 1. On the other hand, if one uses only photometric points at a single epoch, the scatter in the resulting bolometric fluxes (at different epochs) is significant. Typically, the bolometric fluxes measured near the maximum or minimum in the K band, can differ by about 30% from the time–averaged value. This implies a potential bias of up to ≈7% in the effective temperature. Our conclusion is that one should ideally combine angular diameters and bolometric fluxes obtained at the same epoch. If this is not possible, then the best approach is to use a time–averaged bolometric flux, which might lead to a biased temperature but with a relatively small effect (that we have included). In the case of known variability, the use of a single–epoch bolometric flux can lead to smaller formal errors but is subject to a more significant bias.

We have estimated interstellar extinction according to different methods for the K and the M giants in our sample. For all the K giants that are sufficiently nearby, reliable distances are available from Hipparcos, and we have combined them with the extinction maps given by Lucke 1978. Alternatively, the extinction can be estimated on the basis of the observed E(B−V) color excess. These two methods are in general in agreement, except for very nearby stars, where we have preferred the second method, in consideration that the extinction maps may have less reliability on short distances.

In the case of M giants, neither of these approaches is applicable. The stars being further away, only 1/3 of them have

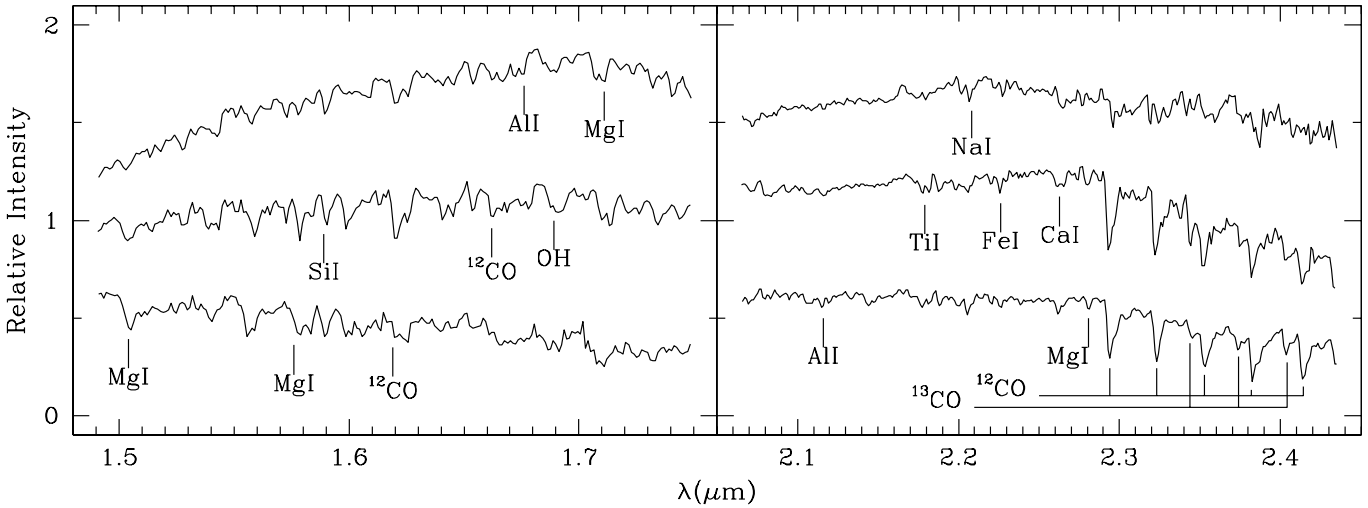

Fig. 3. NIR spectra taken in the H and K bands are shown for selected giants in the spectral range from K0 to M9. From top to bottom, on the left are shown the spectra of AW Tau (M9), Z Cnc (M6) and IRC+20141 (K2). On the right AW Tau (M9), Z Cnc (M6) and IRC+20071 (K5).

Hipparcos distances and then only with a large uncertainty. Additionally, the (B−V) colors are biased by absorption bands. Hence, we had to resort to the following iterative method. Initially, we assumed an absolute luminosity for a given spectral class (e.g. Lang 1991 till M6, and extrapolation thereafter). From this, an initial guess for the distance was estimated from the comparison with the observed luminosity. Using again the extinction maps of Lucke 1978 we could thus determine a value for the extinction. From this, we updated the luminosity and the method was iterated until convergence. The uncertainty involved in this approach is mainly in the assumed absolute luminosity, especially in the case of spectral classes later than M6.

Using these different methods, we have been able to derive the $A_{\rm v}$ values listed in Table 1. Note that the values are relatively small as we are dealing with relatively nearby stars (a necessity if we must be able to resolve their angular diameters). One should consider that in the case of IRC−20307 (the source with the highest $A_{\rm v}$ value, 1.3 mag), if extinction is neglected the resulting bolometric flux would be underestimated by 30%. The $A_{\rm v}$ correction is therefore essential, at least in a significant fraction of cases. Such a correction, however, might introduce a bias if systematic errors in the $A_{\rm v}$ values are present. Note that $A_{\rm v}$ is directly correlated with the resulting bolometric flux.

From a comparison of the values deduced using the different methods described above, we estimate that our $A_{\rm v}$ values have an accuracy of about 0.2 mag. To quantify the error introduced by this uncertainty, we have simulated the change in the bolometric flux of IRC−20307 for a change of ±0.2 mag in the assumed extinction. The result is a difference in absolute value of 6%. This corresponds to a 1.5% variation in the effective temperature, and in addition this must be considered a limiting case because the influence on the flux is proportional to the amount of extinction and is expected to be less important for the other stars in our sample. Thus we conclude that our bolometric fluxes are free from bias due to interstellar extinction.

Note also that circumstellar extinction is present in some of the stars in our sample. However in this case the absorbed photospheric radiation is re-emitted locally, and shows up in the spectral energy distribution as an IR excess. When required, a second black body was fitted to this excess, and this contribution was added to the stellar component, thus yielding the original bolometric flux from the photosphere. On average, we have found IR excesses amounting to about 1% and 9% of the total flux in the spectral ranges M5 to M7 and later than M7, respectively.

3.3. Spectral classification

The spectral classification available in the literature for the stars in our sample was overall satisfactory. In a few cases, however, some possible discrepancies have been noted, such as conflicting determinations, inconsistency with the observed NIR colors or the estimated effective temperature, or unknown original source of classification. Moreover, the spectral class can change during the variability cycle in Mira stars.

In order to avoid any error due to possible misclassification, we have carried out a long-term program in which NIR spectra have been recorded for some selected sources in our sample, as well as for reference stars in order to check our classification scheme. The spectra were taken in the H and/or K band using LonGSp (Vanzi et al. 1997) at the TIRGO 1.5m telescope with a spectral resolution of $\lambda/\Delta\lambda \approx 10^3$. Column (7) in Table 1 lists whether a H and/or K spectrum was recorded. Fig. 3 shows a few sample spectra in the H and K bands.

There is not a general consensus in the literature on spectral–typing criteria at the resolution and wavelength of our spectra, and therefore we did not carry out any detailed line–ratio or equivalent width analysis to classify our spectra. Instead, the shape of the continuum and a few dominant absorption features in our spectra have been compared with spectroscopic standards (Kleinmann & Hall, 1986; Arnaud et al., 1989; Lançon

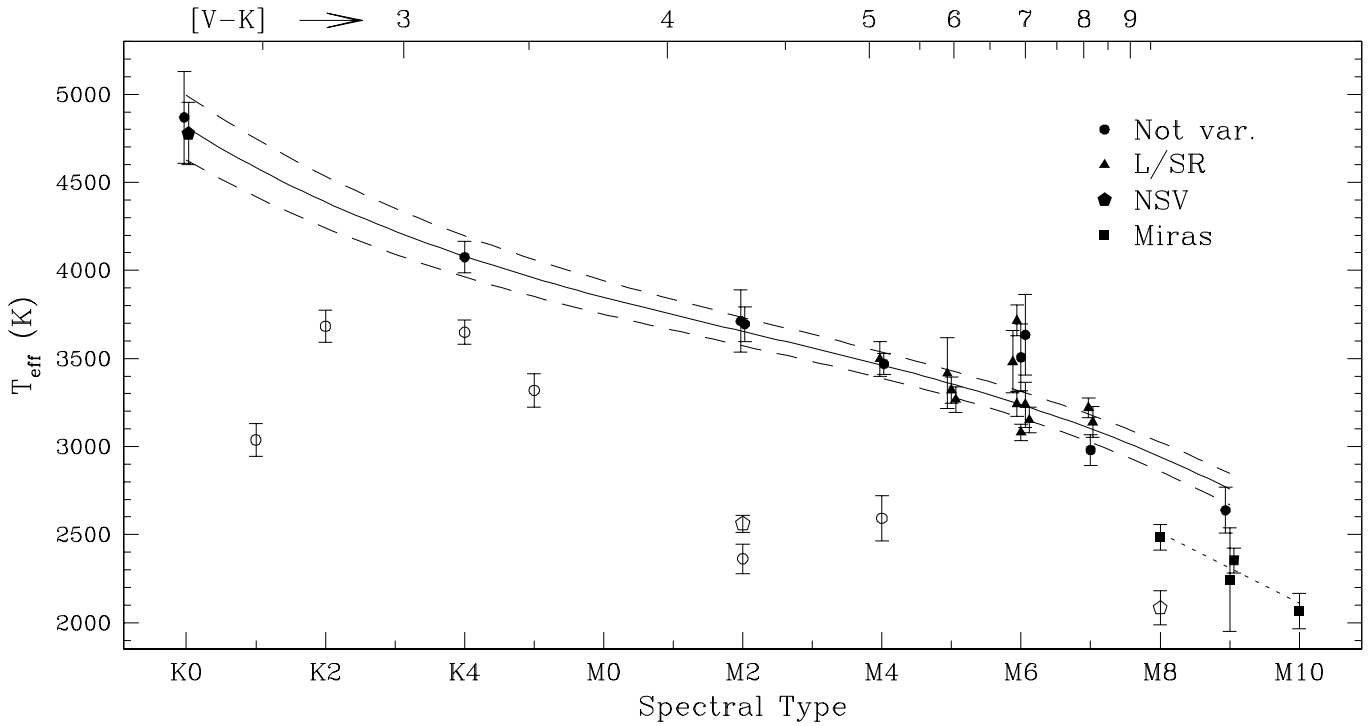

Fig. 4. Effective temperature values for the giant stars in our sample. The symbols refer to the variability class. Our mean calibration is shown as a solid line, while the dashed lines represent the range of the associated error as explained in the text. The stars shown as open symbols were not used in the calibration. Some points are shown slightly displaced from their nominal spectral type position to improve readability. The uncertainties connected to the tentative calibration for the Mira stars (shown as a dotted line) are discussed in the text.

& Rocca-Volmerange, 1992) taken with the same instrument. In particular, the K band spectra of the earliest types considered (K5 to M2) are essentially flat with a slight change in slope at the onset of the $^{12}CO_{(2,0)}$ band-head at 2.29 μm. Later spectral types show an increasingly marked slope and also a stronger absorption by FeI at 2.226 μm. Other lines also become stronger, such as the NaI doublet at 2.208 μm and the CaI triplet at 2.263 μm. Around M5 to M7 the (pseudo) continuum appears to curve more and the strength of the ^{12}CO bands is stronger with respect to the atomic lines. This latter effect is reduced in later types, which however show an even more marked curvature. The H band spectra can be sorted according to similar criteria, although in this case there are fewer useful atomic lines (an example is MgI at 1.504 μm).

Overall these criteria are only accurate to about 2 to 4 subclasses. However the combined use of the H and K bands provides additional reliability and we have been able to make a judgement in 3 cases in which the literature determinations were uncertain or multiple, while a substantial agreement was found in the remaining 9 cases.

4. A revised effective temperature calibration

The data listed in Table 1 are shown in graphical form in Fig. 4. In the figure, different symbols are used to identify the variability class of each source. The open symbols identify stars for which our result appears in strong disagreement with the expected value, and will be discussed separately. They were not used for the calibration (see Table 1). The Mira stars are fitted separately and we will discuss initially the non–Miras only.

In order to derive a mean calibration from effective temperature data, it is customary to plot them as a function of some quantity and fit a reasonable function. There is no standard criterium on which quantity to use for the abscissa in such a plot, or which function should be fitted. It has often been the case in previous similar works, that the temperature is plotted against a color index such as [V–K]. This has the advantage of providing a physical quantity that is easily defined and plotted. Nonetheless, this approach remains arbitrary in practice, because it is not the real color index of each star which is used (this would imply the need for actual measurements at the time of the diameter measurements, since variability is often quite pronounced in the visual bands), but rather some standard color index for the given spectral type. Moreover, color indices such as [V–K] become quickly unreliable as one moves towards cooler spectral types because of the very significant absorption bands that occur in the filter bandpasses. Other indices have been used such as [I–L] which are less subject to absorption, but also in this case the standards may not be universally accepted or even available for the coolest spectral types.

In our case, we have decided to plot and fit T_{eff} against the spectral class. This is easily accomplished in terms of observational data, but presents the disadvantage that the spectral classes do not represent a continuous and accurately measurable physical quantity, and therefore they must be shown in the

plot in an arbitrary way. The data of Fig. 4 are displayed using equally spaced spectral classes. Note also that at the top of the same figure, also the [V–K] index is shown for reference, using the values given in P98.

We note that a different assumption on the spacing of the classes would represent a non-linear scaling of the horizontal axis in the figure. Given the fact that the fit is done using also an arbitrary function, the ambiguity seems inevitable and we are satisfied with the fact that the data appear to be easily fitted with a simple function. In particular, a cubic curve has been used to fit the weighted means of the points available for each spectral class. The fit is satisfactory, and is shown as a solid line in Fig. 4. We have also fitted the weighted means of the extremes of the same data set, and the corresponding dashed lines in the figure can be assumed as the limits of the formal error of the calibration.

The same calibration is shown also in tabular format in Table 2 for ease of reference and comparison to previous works. In the table, our calibration is given in two forms: Column (1) lists the values obtained as a weighted mean of the actual $T_{\rm eff}$ determinations at each subclass, while Column (2) lists the value obtained from the fitting function described above. In the first case the error is taken to be the weighted root mean square of the weighted mean, while in the second case it corresponds to the location of the dashed lines in Fig. 4, as described above. Note that in Column (1), in the cases in which only one star is available for a given spectral type, the error could not be computed. In the case of types M2 and M4, the measurements have a formal error in Column (1) which is very small (5 and 10 K respectively). In view of the approximations used in the estimation of the Rosseland diameters (0.5% in $T_{\rm eff}$, see Sect. 3.1), and of the effects of variability and/or interstellar extinction where applicable (1.5% in $T_{\rm eff}$, see Sect. 3.2), a more realistic estimate of the intrinsic accuracy of our calibration cannot be smaller than about 50 K. In practice, another significant limit is set also by the uncertainty in the spectral classification, as discussed below.

Table 2. Comparison of calibrations ($T_{\rm eff}$ in K)

Sp.	This work (1)	This work (2)	Previous Works R80	Previous Works D96	Previous Works P98
Non–Miras					
K0	4805± 40	4810±185	4790	–	–
K1	–	4585±165	4610	4510	–
K2	–	4390±145	4450	4370	–
K3	–	4225±130	4270	4230	–
K4	4075± na	4080±120	4095	4090	–
K5	–	3955±105	3980	3920	–
M0	–	3845± 95	3895	–	–
M1	–	3750± 85	3810	3835	–
M2	3700± 5	3655± 80	3730	3740	–
M3	–	3560± 75	3640	3675	–
M4	3475± 10	3460± 75	3560	3595	–
M5	3300± 40	3355± 75	3420	3470	–
M6	3230±210	3240± 75	3250	3380	3243±79
M7	3150± 95	3100± 80	–	3210	3087±94
M8	–	2940± 85	–	–	2806±42
M9	2640± na	2755± 90	–	–	–
Miras	(tentative) (1)	(tentative) (2)		VB96 (3)	VB96 (4)
M8	2485± na	2510±(70)		2500	2580±225
M8.5	–	–		2380	2520±280
M9	2350± 25	2310±(85)		–	–
M10	2065± na	2110±(100)		–	–

4.1. Non–Mira stars

For the non–Miras, it can be seen that there is good agreement between our calibration and previous ones such as R80, D96 and P98. We note that these latter two works are based at least in part on interferometric results, and therefore this agreement shows that within the errors the various techniques converge towards the same conclusions. For those parts of the previous calibrations which are based also on lunar occultation, we stress that our determinations are completely independent and do not include any previous result from other groups.

Some additional comments are in order about the coolest spectral types. Firstly, we note that there is some discrepancy between calibrations prior to this work. Specifically, D96 seems in disagreement with P98 at M6 and M7. P98 on the contrary agrees with R80 for M6, but is based on one measurement only. Our calibration seems to agree with R80 and P98 better than with D96 as far as M6 and M7 spectral types are concerned. As for M8, P98 is the only calibration for which a comparison can be made, and we note that the agreement is less good although still consistent within the error bars. Admittedly we do not have specific measurements for non–Miras at M8 (AFGL 5151S has not been considered because of its NSV class, and large amplitude variations which suggest a Mira–like character). Rather we rely on the single measurement at M9, which seems sufficiently reliable and consistent with a natural extrapolation of our fitting curve beyond M7. Note however that as far as the mean relation is concerned, our conclusions depend on the assumed form of the fitting curve and a better agreement with P98 could be obtained by imposing a sharper bend after M6-M7. More measurements at spectral types M8 and M9 are needed to clarify the detailed form of the mean calibration.

4.2. Mira stars

Four Miras stars are present in our sample. Given the limited number, we have chosen to fit their $T_{\rm eff}$ data with a simple straight line, and the result is shown also in Fig. 4. This should be considered only a very tentative attempt to calibrate the $T_{\rm eff}$ relation for Miras, in consideration of the uncertainties in the related phase–dependent quantities as discussed in the following. For the same reason, the associated errors listed in columns (1) and (2) of Table 2 should be considered with care and we

have chosen not to show at all the corresponding error lines in Fig. 4.

The main problem in the calibration of Mira stars is the fact that these stars change spectral subclass and effective temperature during their variability cycle. Both effects are caused essentially by the change of luminosity, whilst the change of Rosseland radius (typically 10 to 20%, e.g. Bessell et al. 1996 and Hofmann et al. 1998) and of atmospheric structure are less crucial but nevertheless non-negligible. In the case of our stars, we do not have specific information relative to the flux and spectra at the time of our diameter measurement, and additionally the phase can be estimated only for R Leo and RU Ari (0.2 in both cases), but not for AW Tau and AFGL 2061 which are much less studied in the literature. We stress that the bolometric fluxes that we have computed for the Miras are based on photometry collected on different dates, and therefore can be considered to reflect a time average. The spectral types, however, are from the literature, and it is not entirely clear whether they should be taken to represent a phase-mean and, if so, how the averaging is performed. Typical variations in the spectra of Mira stars during their cycles are of the order of 2 to 4 subclasses, and therefore quite substantial for the purpose of a $T_{\rm eff}$ calibration. As a result, the conclusions that we can derive about the effective temperatures of the Miras stars in our sample are only very tentative. Nevertheless they represent a substantial extension to the available data and as such we report them.

Van Belle et al. (1996, VB96 hereafter) have presented a new calibration of Mira variables that indicates that Miras of given spectral types measured in terms of TiO and VO band strengths (Lockwood & Wing 1971, Lockwood 1972) are ≈ 350 K cooler than non-Miras of the same type. Inspection of their Fig. 1 shows, however, that there is no substantial overlap of Miras and non-Miras around M6 and that, also in consideration of the large temperature scatter seen in this diagram, other interpretations would also be justified. In fact, some models suggest that Mira stars should exhibit stronger TiO bands, i.e. later spectral types, than non-Miras at effective temperatures around and somewhat below 3000 K (Bessell et al. 1989b, 1996) in agreement with TiO index vs. color temperature observations (see Figs. 10 and 11 of Bessell et al. 1996). The fact that the Miras temperatures that we derive appear to follow naturally the $T_{\rm eff}$ relation for non–Miras but with an offset of about 400 K seems to confirm the finding of VB96, but probably a more systematic study covering a wide range of Mira parameters and phases should be carried out to clarify this point. We note that in spite of the uncertainties listed above, all our Mira stars fall below the mean relation of non–Miras, although the small number statistics does not guarantee that this is not a chance case.

In Table 2 we have listed the Mira data separately. In columns (1) and (2) we report our values in the same way as explained for the non–Miras. We report the VB96 fitted and mean results in columns (3) and (4) respectively. The agreement with VB96 is good at M8, and can be considered consistent also at M8.5 (binned type in VB96) by interpolating with our M9 result. We should also mention that for spectral type M10 which is defined by R Cas at minimum phase in the TiO/VO-band classification, new speckle observations of this Mira variable indicate an effective temperature of 1900±150 K (K.-H. Hofmann, private communication), which is in agreement within the given errors with our determination.

4.3. Discussion

It is important to note that for the present calibration, as well as in previous works, possible errors in the spectral classification are neglected. However, we have illustrated in Sect. 3.3 that an error of one subclass or even more is indeed possible. From the data presented in Table 2, it can be seen that the $T_{\rm eff}$ change from one subclass to the next is in the range 100 to 150 K for the M giants, so that errors in the spectral classification have the potential to limit dramatically the accuracy of the calibration. At the present stage one cannot quantify this effect more precisely, and has to rely on the hope that the distribution of such errors is gaussian and might cancel out when sufficiently large numbers of stars are considered. This would be expecially true if larger databases of angular diameters became available, which should become feasible as more sensitive and accurate long–baseline interferometers come into operation, or if wider effort to record LO events are undertaken.

We turn now our attention to the discrepant points in Fig. 4, identified by open symbols. There are 7 such sources in the spectral range K1 to M4, which appear to have an associated effective temperature about 900 K lower than the mean expected value (we do not include AFGL 5151S at M8 for the reasons given above). Although we do not have a definitive explanation, several possibilities can be speculated. The fact that all these discrepant sources fall below the effective temperature scale –and none above it– could lead one to argue that we have overestimated the angular diameter, a typical bias when observational effects (such as scintillation or instrumental characteristics) are not properly accounted for in the data reduction. To our knowledge however, we have very carefully included all such effects in our data reduction scheme, and fits using smaller angular diameters appear to be inconsistent with the data. Additional independent observations of these sources would be required to clarify the matter. Also an underestimated bolometric flux could produce a lower effective temperature. However, this possibility seems remote since in many of the discrepant cases our bolometric fluxes are based on repeated photometric measurements of good quality. Note that in two cases, namely IRC+20141 and IRC+20071, we quoted in the past bolometric fluxes ≈60% higher (Richichi 1998a). However, these were obtained in the absence of JLM photometry, replaced by empirical estimates, and as a consequence the interstellar extinction was subject to a large uncertainty. For this work, we used a wider set of photometric values and a consistency check on the extinction.

The presence of a close secondary component at a distance of a few milli-arcseconds could mimic a larger diameter. However, we do not expect such a large fraction of giants to have close secondaries of suitable brightness. Effects such as abnormal metallicity, star spots, asymmetric brightness profiles could also partially explain the discrepancy, but not fully. It is possi-

ble that the combination of more than one above mentioned effects could produce the observed discrepancy, but at the moment we must conclude that no simple definitive explanation can be provided and we must leave the question open to further investigations. We note that previously also Dyck et al. 1998 have reported ≈9% of giants stars in their sample showing an effective temperature about 750 K below the mean expected value, for which no immediate explanation could be found.

5. Conclusion

We have presented an effective temperature scale for the K and M type normal giants which for the first time extends to M9 spectral class. The temperature scale presented here is based on our homogeneous database of 34 lunar occultation light curves collected over a period of more than a decade, complemented by photometry and spectroscopy which are partly from the literature and partly original. The lunar occultation data have been re-analyzed to express the angular diameters in terms of the Rosseland radius, a physically meaningful quantity that can be directly compared to theoretical model predictions. The conversion factor to obtain this radius from the uniform disk radius has been established as a function of the spectral type by using for the first time a grid of center-to-limb variation models to fit the observed occultation light curves.

The derived temperature scale is consistent in the region of overlap with the earlier calibrations by Ridgway et al. 1980 (based on lunar occultations only) and by Dyck et al. 1996 (D96) and by Perrin et al. 1998 (P98) (based largely on interferometric data). For the spectral types M6 and M7, our calibration shows better agreement with the cooler temperatures inferred by P98, although some marginal agreement with D96 could also be justified. We stress that more effective temperature determinations for the spectral classes M8 and M9 are required to clarify the details of the calibration, and to discriminate significantly between the conclusions of different authors.

Included in our sample are also 4 Mira stars in the spectral range M8 to M10. A tentative calibration shows agreement with the results of Van Belle et al. 1996, and with their finding that Miras appear to exhibit effective temperatures significantly lower than non-Miras of the same spectral type. However this aspect is not entirely clear from the theoretical point of view, and at least as our data are concerned the uncertainties related to the spectral and photometric variability are sufficient to caution against firm conclusions. Further theoretical investigations as well as detailed observations of Mira stars at several pulsational phases are needed to reach a convincing effective temperature calibration.

Finally, we note that seven stars in our sample appear to display effective temperatures significantly lower (on average 900 K) than the mean relation. We have not been able to find a simple explanation for this in terms of possible observational or analysis biases, and we remark that similar discrepant cases were noted also by Dyck et al. 1998.

Acknowledgements. This research has made use of the *Simbad* database, operated at CDS, Strasbourg (France). A.R. has been partially supported in his work by a Chretien Grant awarded by the American Astronomical Society. We thank the referee, Dr. T. Bedding, for his comments and his help in improving the presentation.

References

Arnaud K.A., Gilmore G., Cameron A.C., 1989, MNRAS 237, 495
Barnes T.G., Evans D.S., 1976, MNRAS 174, 489
Baschek B., Scholz M., Wehrse R., 1991, A&A 246, 374
Bessell M.S., Brett J.M., Scholz M., Wood P.R., 1989a, A&AS 77, 1 (erratum: 87, 621)
Bessell M.S., Brett J.M., Scholz M., Wood P.R., 1989b, A&A 213, 209
Bessell M.S., Brett J.M., Scholz M., Wood P.R., 1991, A&AS 89, 335
Bessell M.S., Scholz M., Wood P.R., 1996, A&A 307, 481
Di Benedetto G., Rabbia Y., 1987, A&A 188, 144
Di Giacomo A., Richichi A., Lisi F., Calamai G., 1991, A&A 249, 397
Dyck H.M., Benson J.A., van Belle G.T., Ridgway S.T. (D96), 1996, AJ 111, 1705
Dyck H.M., van Belle G.T., Thompson R.R., 1998, AJ 116, 981
Hofmann K.-H., Scholz M., 1998, A&A 335, 637
Hofmann K.-H., Scholz M., Wood P.R., 1998, A&A 339, 846
Kleinmann S.G., Hall D.N.B., 1986, ApJS 62, 501
Lançon A., Rocca-Volmerange B., 1992, A&AS 96, 593
Lang K.R., 1991, In: Astrophysical data: Planets and stars. Springer publishers, Berlin
Lockwood G.W., 1972, ApJS 24, 375
Lockwood G.W., Wing R.F., 1971, ApJ 169, 6
Lucke P.B., 1978, A&A 64, 367
Perrin G., Coudé du Foresto V., Ridgway S.T., et al. (P98), 1998, A&A 331, 619
Richichi A., Salinari P., Lisi F., 1988, ApJ 326, 791
Richichi A., Lisi F., 1990, A&A 230, 355
Richichi A., Lisi F., Di Giacomo A., 1992a, A&A 254, 149
Richichi A., Di Giacomo A., Lisi F., Calamai G., 1992b, A&A 265, 535
Richichi A., Calamai G., Leinert Ch., et al., 1996a, A&A 309, 163
Richichi A., Baffa C., Calamai G., Lisi F., 1996b, AJ, 112, 2786
Richichi, A. Calamai G., Leinert Ch., Stecklum B., 1997, A&A 322, 202
Richichi A., Ragland S., Fabbroni L., 1998a, A&A 330, 578
Richichi A., Ragland S., Stecklum, B., Leinert Ch., 1998b, A&A in press
Ridgway S.T., Joyce R.R., White N.M., Wing R.F. (R80), 1980, ApJ 235, 126
Samus N.N. (Ed.), 1990, General Catalog of Variable Stars. $4^{\rm th}$ edition, Vol. IV, Nauka, Moscow
Schmidtke P.C., Africano J.L., Jacoby G.H., Joyce R.R., Ridgway S.T., 1986, AJ 91, 961
Scholz M. 1997, In: Bedding T.R., Booth A.J., Davis J. (eds.) IAU Symp.189 on Fundamental Stellar Properties. Kluwer, Dordrecht, p. 51
Scholz M., Takeda Y., 1987, A&A 186, 200 (erratum: 196, 342)
van Belle G.T., Dyck H.M., Benson J.A., Lacasse M.G. (VB96), 1996, AJ 112, 2147
Vanzi L., Sozzi M., Marcucci G., 1997, A&AS 124, 573